Study of the first step of the Mn_2O_3/MnO thermochemical cycle for solar hydrogen production

Javier Marugán[1], Juan A. Botas[2,*], Mariana Martín[3], Raúl Molina[1], Carolina Herradón[2]

[1]*Department of Chemical and Environmental Technology, Rey Juan Carlos University, c/ Tulipán, s/n, 28933, Móstoles, Spain*

[2]*Department of Chemical and Energy Technology, Rey Juan Carlos University, c/ Tulipán, s/n, 28933, Móstoles, Spain*

[3]*Hynergreen Technologies, S.A., Campus Palmas Altas, 41012, Sevilla, Spain*

(*) corresponding author: Tel.: +34 91 488 7008; fax: +34 91 488 7068; E-mail address: juanangel.botas@urjc.es

Published on

International Journal of Hydrogen Energy 37 (2012) 7017–7025.

doi:10.1016/j.ijhydene.2011.10.124

Abstract

In this work, a complete thermodynamic study of the first step of the Mn_2O_3/MnO thermochemical cycle for solar hydrogen production has been performed. The thermal reduction of Mn_2O_3 takes place through a sequential mechanism of two reaction steps. The first step (reduction of Mn_2O_3 to Mn_3O_4) takes place at temperatures above 700 ºC, whereas the second reaction step (reduction of Mn_3O_4 to MnO) requires temperatures above 1350 ºC to achieve satisfactory reaction rates and conversions. Equilibrium can be displaced to lower temperatures by increasing the inert gas/Mn_2O_3 ratio or decreasing the pressure. The thermodynamic calculations have been validated by thermogravimetric experiments carried out in a high temperature tubular furnace. Experimental results corroborate the theoretical predictions although a dramatically influence of chemical kinetics and diffusion process has been also demonstrated, displacing the reactions to higher temperatures than those predicted by thermodynamics. Finally, this work demonstrates that the first step of the manganese oxide thermochemical cycle for hydrogen production can be carried out with total conversion at temperatures compatible with solar energy concentration devices. The range of required temperatures is lower than those commonly reported in literature for the manganese oxide cycle obtained from theoretical and thermodynamic studies.

Keywords: Thermochemical water splitting, Hydrogen production, Manganese oxide

1. Introduction

Nowadays, the world faces an energy crisis mainly caused by the depletion of conventional resources and increasing environmental problems produced by the use of fossil fuels. Thus, increasingly ambitious policy targets to reduce greenhouse gas emissions as well as the need of sustainable energy system have created a need for alternative fuels and energy sources [1].

In this context, hydrogen has been proposed for decades as a promising energy carrier for a future low carbon energy economy. Hydrogen can be generated from many energy sources, including reforming of natural gas or gasification of coal [2]. However these routes for hydrogen economy do not release the world from the fossil fuel dependence so a massive hydrogen use is reasonable only if renewable energy sources are used for its production. In this sense, direct splitting of water using solar concentrated solar energy is the most direct and clean method to obtain hydrogen (reaction 1).

$$H_2O \rightarrow H_2 + ½\ O_2 \qquad (1)$$

However, from a practical viewpoint this reaction implies significant difficulties derived of the required high temperatures. According to Perkins and Weimer a value of zero for ΔG_r (Gibbs free energy of the reaction) is reached only at temperatures of ca. 4250 ºC [3], whereas Kogan and co-workers showed that even at temperatures of 2250 ºC only a 25 % of dissociation of the water can be reached [4].

Temperatures as high as 1500-1600 ºC are possible to be achieved in modern solar concentrating systems with concentration factors in the range of 1500-5000. However, this value is far from 2250 ºC and there are also inherent problems associated to this technology. First of all, selection of the material for the reactor becomes a critical point in the design of the system. Secondly, it is necessary to separate the hydrogen and the oxygen at that temperature in order to avoid recombination at lower temperature or the formation of explosive mixtures when reducing the temperature. Some research has been done on this field, such as the design of porous ceramic membranes semi permeable to O_2 or H_2 [5-7], although the gas flow rates are considerable low and the sintering of the porous structure at such high temperatures reduce their permeability. Other alternatives, such as palladium-based

membranes for H_2 and catalytic membranes for oxygen separation have been also tested, although the application is limited to temperatures in the range of 530-870 ºC [8, 9]. Finally, higher temperature implies higher radiation losses in a solar collector system, since it is proportional to the fourth power of absolute temperature, with a direct impact in the efficiency of the water splitting process.

For those reasons, water splitting by solar-driven thermochemical cycles represents a promising technology to reduce the extremely high temperatures of the direct water splitting. Thermochemical cycles involve two or more steps in which a solid oxide is thermally reduced and oxidized, being the net result of all of them the dissociation of water (reaction 1), although it occurs through two or more endo- and exothermic reactions with lower temperature requirements. There are more than 200 thermochemical cycles reported in literature although only 14 have been selected as the more promising for solar hydrogen production, according to different criteria, such as cost, degree of development, environmental risk or energy efficiency [10, 11]. Among all of them, the metallic oxides cycles of 2 or 3 steps have been the most attractive thermochemical cycles for coupling with concentrated solar thermal energy. Two steps metallic oxide cycles involve a first process in which the metallic oxide is reduced at high temperature with release of O_2 and a second process in which the metal reacts with water to form H_2 and regenerating the metallic oxides. Fe_3O_4/FeO, Zn/ZnO, SnO/SnO_2 and CeO_2/Ce_2O_3 are examples of redox systems that have been studied in the literature [12-16]. Despite their apparent simplicity, the temperatures required for the reduction step are still really high (1630-2270 ºC) and although a solar reactor has been successfully used in the laboratory for the dissociation of ZnO at 1700 ºC [17], several studies have diverted attention to different alternatives to decrease the temperature required for the process. Researches have proposed mixed metallic oxide redox pairs, mainly based on iron oxide, to reduce the temperature of the Fe_3O_4/FeO cycle. Thus, partial substitution of iron for other metals (Ni, Zn, Cu, Co, Mn) to form spinel ferrites leads to temperatures of the reduction steps of 1340-1500 ºC, as compared to the temperature of the initial cycle, around 2230 ºC [18, 19]. Moreover, supporting of the ferrite over zirconia has been proposed as an alternative to not only reduce the temperature of the system but a better absorption of energy irradiation in the solar set-up [20, 21]. Similar temperature of operation were achieved when doping CeO_2 with zirconia and other metals [22] and it is even lower whit $Ce_{1-x}Pr_xO_{2-\delta}$ ceramic materials [23].

A different approach is the study of thermochemical cycles based on more than two steps, which require lower temperatures [24]. Sturzenegger and Nüesch proposed in 1999 a new manganese-oxide-based cycle for the production of solar hydrogen [25]. This cycle consists of three steps (reactions 2 - 4) in which the Mn_2O_3 is reduced to MnO that can react with NaOH, producing $NaMnO_2$ and releasing hydrogen. The final step would be the regeneration of the initial Mn_2O_3 and the NaOH employed to close the reaction cycle.

$$Mn_2O_3 \rightarrow 2\ MnO + ½\ O_2 \qquad (2)$$

$$MnO + NaOH \rightarrow NaMnO_2 + ½\ H_2 \qquad (3)$$

$$NaMnO_2 + ½\ H_2O \rightarrow ½\ Mn_2O_3 + NaOH \qquad (4)$$

Early papers were focused on theoretical analysis of the efficiency of the cycle [25], whereas more recent studies report experimental data that prove the feasibility of the essential high temperature reduction step [26].

The thermal reduction of Mn_2O_3 into MnO occurs through two reaction steps (5 and 6). Theoretically, the overall reduction step occurs at temperatures above 1560 ºC [25], and it could be provided by thermal solar energy in a concentrator device.

$$Mn_2O_3 \rightarrow 2/3\ Mn_3O_4 + 1/6\ O_2 \qquad (5)$$

$$2/3\ Mn_3O_4 \rightarrow 2\ MnO + 1/3\ O_2 \qquad (6)$$

A recent study has reported the thermal reduction of manganese oxide in a high-temperature aerosol reactor (AFR) [26]. This type of diluted particle phase reactor has shown to yield high dissociation reaction rates using other metal oxide systems. The temperature required for the first step of the process was varying from 1400 to 1600 ºC and the possible recombination of the released oxygen with MnO or Mn_2O_3 regenerating the initial manganese oxide was thoroughly studied. The same authors proposed in other work an alternative method to reduce the operation temperature based on mixed manganese/metal oxides [27]. In this way, the aim of present work is to provide a thorough study of the first step of the Mn_2O_3/MnO cycle, obtaining an accurate range of temperatures in which reactions 5 and 6 are favoured and

studying the effect of this and other variables (pressure and gas phase composition) in the extent of each reaction.

2. Materials and methods

2.1. Materials

Commercial pure manganese oxides (Mn_2O_3, Mn_3O_4 and MnO) were purchased from Sigma Aldrich and used without further treatment.

2.2. Equilibrium calculations

Equilibrium compositions as a function of temperature have been calculated following standard thermodynamic methods. Coefficients of the temperature dependence equation of specific heat at constant pressure (C_P) and values for the standard enthalpies of formation (ΔH_f^o), standard Gibbs energies of formation (ΔG_f^o), and the derived standard entropies of formation (ΔS_f^o) of solid Mn_2O_3, Mn_3O_4 and MnO and gaseous O_2 were obtained from the Aspen Plus® databases. Equilibrium constants (K_P) of the reactions at constant pressure as a function of temperature where calculated from the values of the Gibbs energy of reaction (ΔG_r) computed from the standard enthalpies and entropies of formation and the temperature dependence of the specific heat of the species according to the following equations:

$$K_P = \exp\left(\frac{-\Delta G_r^T}{RT}\right) = \exp\left(\frac{-\Delta H_r^T + T\Delta S_r^T}{RT}\right) \quad (7)$$

$$\Delta H_r^T = \Delta H_r^0 + \int_{T_0}^{T} \Delta C_P(T)\, \mathrm{d}T \quad (8)$$

$$\Delta S_r^T = \Delta S_r^0 + \int_{T_0}^{T} \frac{C_P(T)}{T}\, \mathrm{d}T \quad (9)$$

$$\Delta H_r^0 = \sum_{i=products} \sigma_i \left(\Delta H_f^0\right)_i - \sum_{i=reactants} \sigma_i \left(\Delta H_f^0\right)_i \quad (10)$$

$$\Delta S_r^0 = \sum_{i=products} \sigma_i \left(\Delta S_f^0\right)_i - \sum_{i=reactants} \sigma_i \left(\Delta S_f^0\right)_i \quad (11)$$

$$\Delta C_P(T) = \sum_{i=products} \sigma_i \left(C_P(T)\right)_i - \sum_{i=reactants} \sigma_i \left(C_P(T)\right)_i \quad (12)$$

where σ_i represents the stoichiometric coefficients. Once computed K_P, the evolution of a initial mixture Mn_2O_3:Mn_3O_4:MnO:O_2:N_2 to the equilibrium compositions at a constant pressure (P_T) has been calculated. The molar amount of O_2 that has appeared trough the reaction ($N_{O_2}^{rq}$) is obtained from the difference between the initial amount of O_2 ($N_{O_2}^{0}$) and its equilibrium amount ($N_{O_2}^{eq}$), computed from the reaction equilibrium constant through the partial pressure and the gas composition at the equilibrium ($P_{O_2}^{eq}$ and $y_{O_2}^{eq}$, respectively) as follows:

$$P_{O_2}^{eq} = \left(K_P\right)^{\frac{1}{\sigma_{O_2}}} \tag{13}$$

$$y_{O_2}^{eq} = \frac{P_{O_2}^{eq}}{P_T} \tag{14}$$

$$N_{O_2}^{eq} = N_{N_2} \frac{y_{O_2}^{eq}}{1 - y_{O_2}^{eq}} \tag{15}$$

$$N_{O_2}^{rq} = N_{O_2}^{0} - N_{O_2}^{eq} \tag{16}$$

Finally, the molar amount of the solid phases at the equilibrium has been calculated from the reacted O_2 according to the stoichiometry of the reaction. For instance for reaction (5) the following expressions has been used:

$$N_{Mn_2O_3}^{eq} = N_{Mn_2O_3}^{0} - \frac{\sigma_{Mn_2O_3}}{\sigma_{O_2}} N_{O_2}^{rq} \tag{17}$$

$$N_{Mn_3O_4}^{eq} = N_{Mn_3O_4}^{0} + \frac{\sigma_{Mn_3O_4}}{\sigma_{O_2}} N_{O_2}^{rq} \tag{18}$$

2.3. Thermogravimetric experiments

Thermogravimetric measurements were performed in a TGA/DSC1 STARe System (Mettler, Toledo) with a maximum operation temperature of 1600 °C. The experiments were carried out under nitrogen flow (50 cm^3/min), to keep an inert environment around the Mn_2O_3 sample (50 mg) placed in a platinum crucible of 0.15 cm^3 of total volume (0.11 cm^3 of free gas

volume once the sample is placed inside). The temperature programme consists of different steps. Firstly the TG was ramped up to 150 °C with a heating rate of 20 °C/min and this temperature was kept constant for 30 minutes. This step is used to remove water traces in the sample. Then, the temperature was risen up to the required value ranging from 550 to 1500 °C, with a heating rate of 20 °C/min. Next, isothermal conditions were kept for four hours to measure the weight loss which takes place as a consequence of the thermal reduction and releasing of O_2 to the gas phase. Finally, the TG was cooled down to 40 °C with a rate of 10 °C/min.

2.4. Reactions in a high temperature tubular furnace

Thermochemical experiments were also carried out using a 40-fold higher amount of solid reactant (2 g of Mn_2O_3) in a high temperature tubular furnace. Experimental conditions (heating rate, isothermal program, Q_{N2}/Mn_2O_3 ratio, etc) were the same than those used in TG experiments. Solids at the end of the reaction have been analyzed by X-Ray diffractometry using a Philips PW3040/00 X'Pert MPD/MRD equipment.

3. Results and Discussion

3.1. Thermodynamic study

Some preliminary thermodynamic studies of the Mn-oxide cycle have been already reported in the literature, existing significant discrepancies in their conclusions about the temperatures in which the reactions 5 and 6 proceed and the coexistence of the different solid phases involved (Mn_2O_3, Mn_3O_4 and MnO). Perkins and Weimer published in 2004 a thermodynamic study performed using the *FACT* software (*Facility for the Analysis of Chemical Thermodynamics*, from McGill University) to predict the equilibrium composition of the different solid phases of the first step of the cycle as a function of the temperature [3]. The authors concluded that the thermal reduction of the Mn_2O_3 occurs through two sequential chemical reactions (5 and 6) with no coexistence of the three solid phases at the same time. The first transformation, Mn_2O_3 into Mn_3O_4, starts at 675 ºC and it is completed at 875 ºC. After that, the second reaction, Mn_3O_4 to MnO, takes place between 1475 and 1575 ºC. However, Charvin and co-workers reported a completely different equilibrium composition

with the temperature in 2007 [24]. In that case, the *HSC chemistry 6.1* software (from Outotec Research Oy) was employed, minimizing the Gibbs energy of the reactions to obtain the equilibrium composition. The results obtained show that both reactions take place in a really wide range of temperature. The first transformation starts below 500 ºC and the second transformation at 800 ºC, and both reactions coexist and run simultaneously even at temperature higher than 1800 ºC, leading to a conversion of 95% at 2000 ºC. Obviously, in that case the three phases of manganese oxide will be present at the same time in the process for temperatures above 800 ºC.

In order to put some light in this controversy, a new thorough thermodynamic study of the process has been carried out following the method described in section 2.2. First of all, the thermodynamic equilibrium composition of mixtures of Mn_2O_3, Mn_3O_4, MnO and oxygen were calculated under similar conditions that those used in literature (a pressure of 1 atm and inert gas/solid ratio of 1). According to predicted equilibrium compositions (Figure 1), the first thermal reduction step (reaction 5) takes place between 650 and 770 ºC, whereas the second reduction step (reaction 6) occurs between 1450 and 1500 ºC. Consequently, both reactions seem to be sequential, and MnO is formed only when all the Mn_2O_3 has been reduced to Mn_3O_4. Those results are in agreement with the work of Perkins and Weimer [3], with similar estimated temperatures, especially for reaction 6. In contrast, the temperature in which a total conversion of the second reaction is achieved is almost 450 ºC lower than that predicted by Charvin and co-workers [24].

Equilibrium composition is strongly influenced by the operation variables. Figure 2 show the influence of the pressure on the process. It is clearly evident that the lower the pressure, the lower the required reaction temperature. Particularly, the temperature values necessary for both reactions at 0.1 bar are 100 ºC lower than those necessary at 1 bar, whereas a similar shift to higher temperatures is obtained at 10 bar. Similar behaviour was reported by Charvin and co-workers [24], although in that case the effect was even more significant than that obtained in the present study.

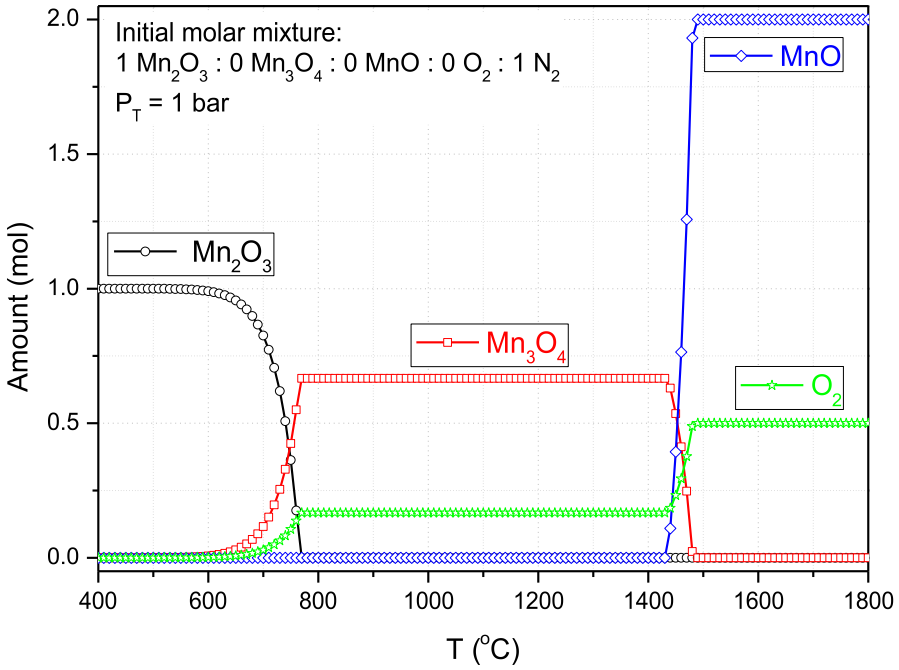

Figure 1. Influence of temperature on the thermodynamic equilibrium of the solid phases of the first step of the Mn_2O_3/MnO thermochemical cycle at 1 bar of total pressure and a ratio inert gas/solid of 1.

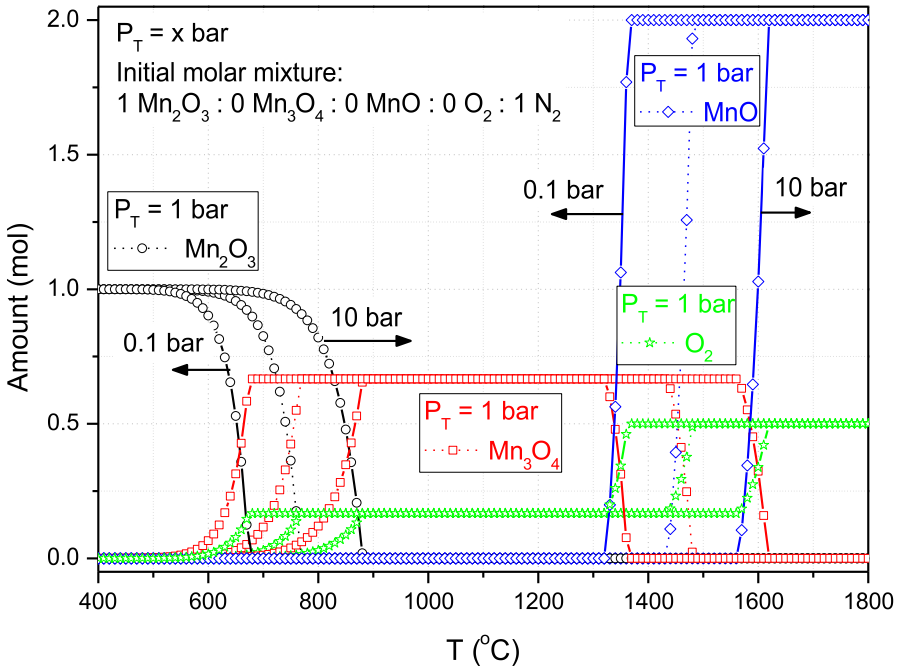

Figure 2. Effect of total pressure in the thermodynamic equilibrium of the solid phases of the first step of the Mn_2O_3/MnO thermochemical cycle at a ratio inert gas/solid of 1.

The influence of the inert gas/Mn_2O_3 molar ratio was also established by calculation of equilibrium composition corresponding to 1 mol of Mn_2O_3 with 0.1, 1 and 10 mol of N_2, at 1 bar (Figure 3). An increase of the inert gas/solid molar ratio displaces the equilibrium to lower temperatures. Thus, similar decrease in the temperatures of the reactions is obtained at 1 bar and a gas/solid molar ratio of 10 or at a pressure of 0.1 bar and a gas/solid ratio of 1. Consequently a technical and economical optimization would be probably required to determine the combination of pressure and inert gas flow that minimizes the total cost, considering the vacuum and energy requirements, and the production and recovery costs of the inert gas.

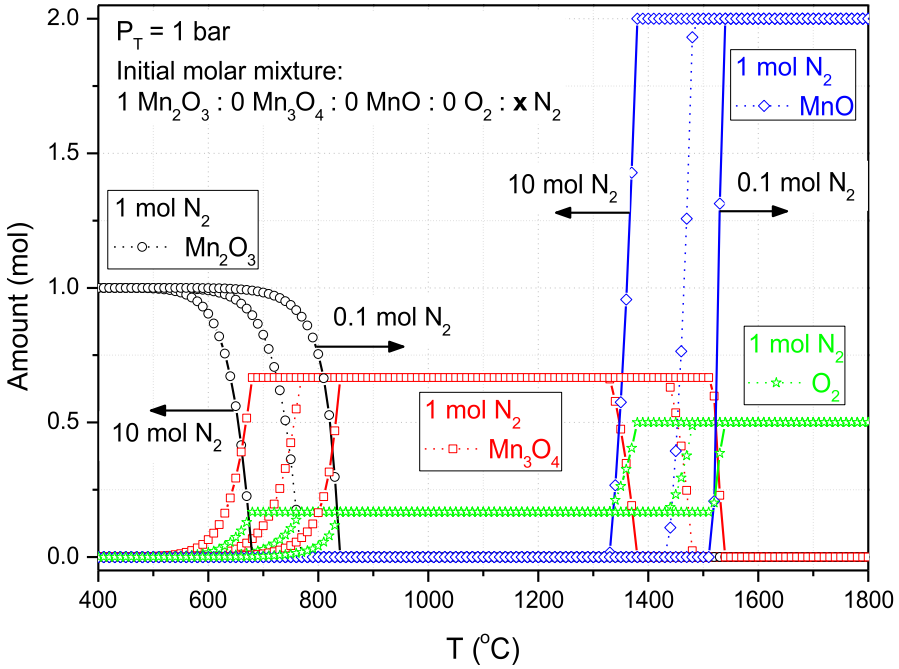

Figure 3. Influence of the gas/solid molar ratio in the thermodynamic equilibrium of the solid phases of the first step of the Mn_2O_3/MnO thermochemical cycle at 1 bar of total pressure.

The use of inert gas is usually considered in the operation of thermochemical cycles as a carrier for the oxygen and the hydrogen generated in the first and second stage of the process, respectively. However, a remarkable decrease in the operation costs will be obtained by changing the inert gas (usually nitrogen or argon) by air. This would eliminate the need for separation of the O_2 to recycle the inert gas. Figure 4 show the equilibrium calculations of the first step of the manganese oxide cycle in presence of a N_2-O_2 mixture (95 % N_2 and 5 % O_2) and air (79 % N_2 and 21 % O_2).

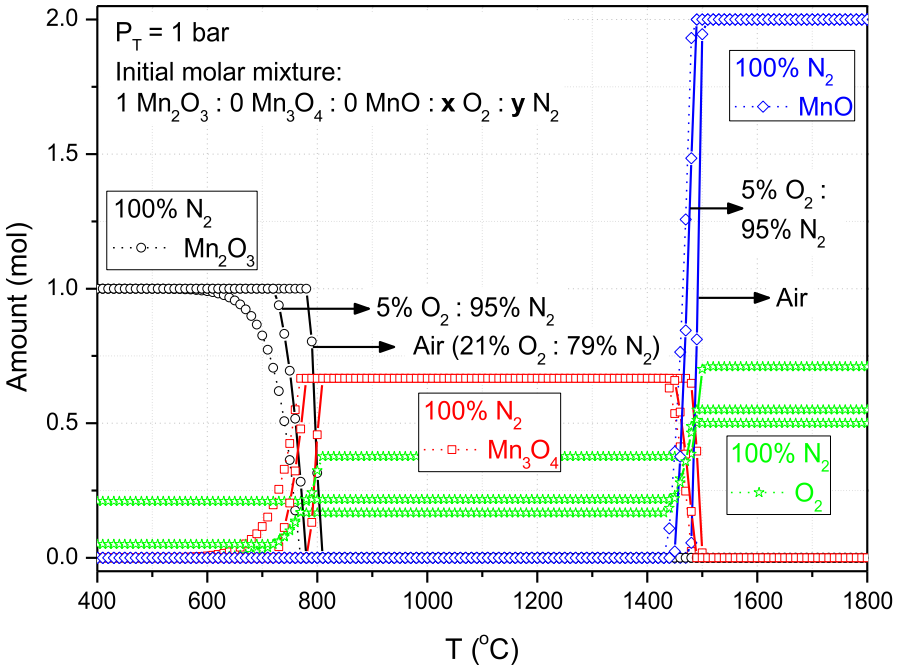

Figure 4. Influence of the O_2 concentration in the gas phase in the thermodynamic equilibrium of the solid phases of the first step of the Mn_2O_3/MnO thermochemical cycle at 1 bar of total pressure and a gas/solid molar ratio of 1.

As it can be seen, the presence of oxygen induces a significant increase in the temperature value in which the first reaction begins, but only a slight increase in the temperature for total conversion, narrowing the temperature range in which the reaction takes place. At this point, it must be noticed that the equilibrium calculations consider an inert gas phase only for the first step (reaction 5), as the oxygen removed during reaction 5 is present in the equilibrium calculations of reaction 6. For that reason a simple approach to shift the second reaction step to lower temperatures could be purging the gas phase with new inert gas at intermediate temperature values (e.g. 1100 ºC), as simulated in Figure 5. Under those conditions, the reduction of Mn_3O_4 to MnO starts at 1300 ºC, instead of 1425 ºC, although the theoretical complete conversion is obtained at 1475 ºC in both cases. In any case, a rigorous approach of the process in the presence of O_2-N_2 mixtures at high temperature should consider the possible formation of NO_x, as shown by Perkins and Weimer [3].

In summary, from all the previous results, it can be concluded that presence of air instead nitrogen does not affect dramatically the temperatures in which the first step of the manganese oxide termochemical cycle proceeds, whereas low pressures and high air/solid ratios seem to be a good choice to reduce the temperatures of reactions 5 and 6. Figure 6 shows the

thermodynamic simulation of the process performed according to those premises, showing that reaction 5 is completed in a range of temperatures of only 650 to 700 ºC, whereas reaction 6 takes place at temperature around 1350 ºC.

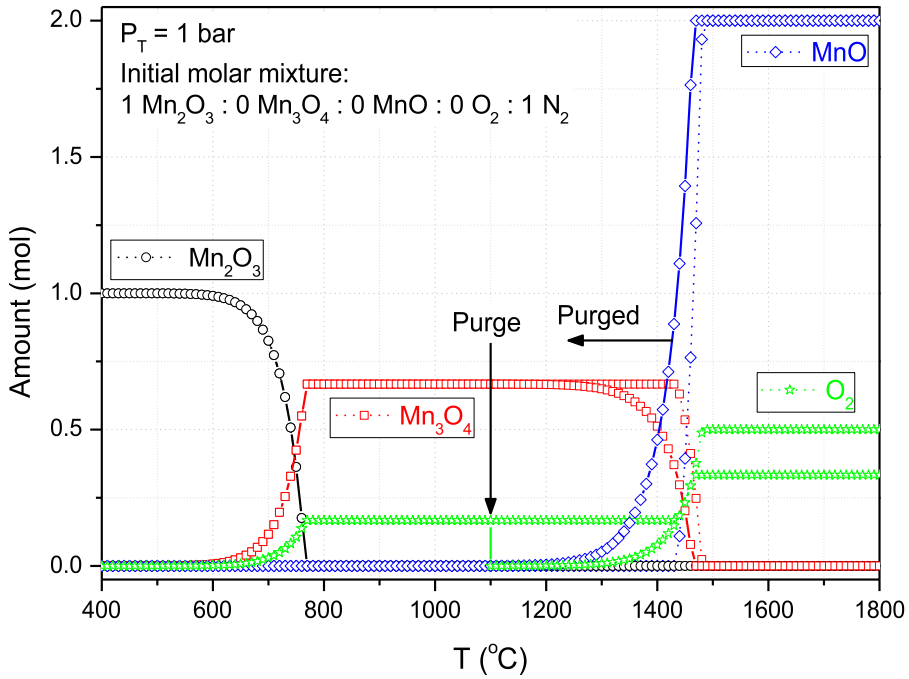

Figure 5. Effect of an intermediate purge with N_2 in the thermodynamic equilibrium of the solid phases of the first step of the Mn_2O_3/MnO thermochemical cycle at 1 bar of total pressure and a gas/solid molar ratio of 1.

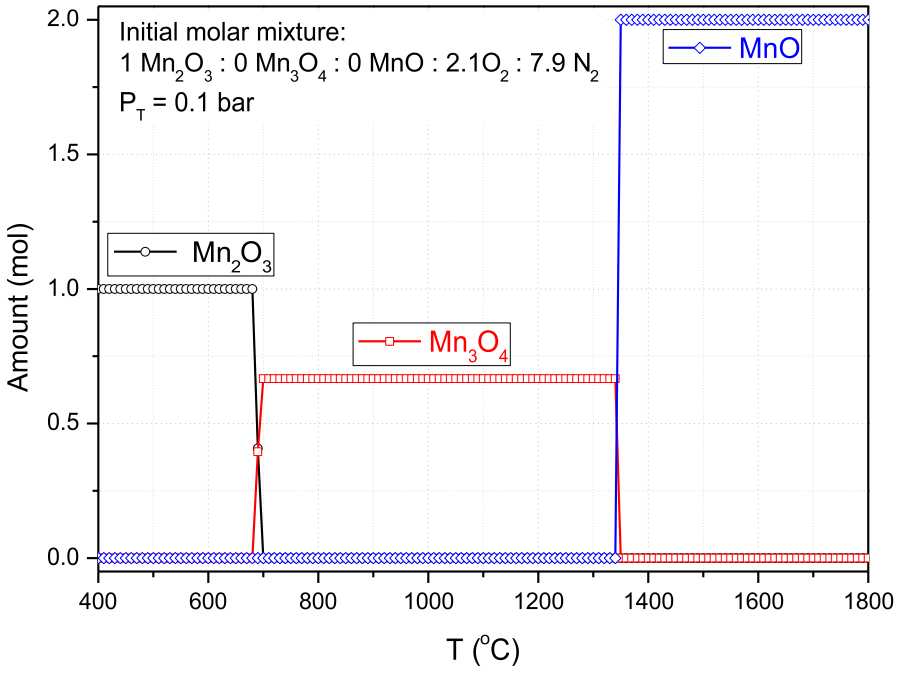

Figure 6. Thermodynamic equilibrium of the solid phases of the first step of the Mn_2O_3/MnO thermochemical cycle in air at 0.1 bar of total pressure and a gas/solid molar ratio of 10.

3.2. Validation of the thermodynamic calculations by thermogravimetric analysis

Validation of the previous thermodynamic calculations has been carried out in a thermobalance, registering the evolution of O_2 released during the thermal reduction of Mn_2O_3 to MnO through the weight loss of the initial solid sample along a defined temperature program. First of all, the first step of the process (reaction 5) has been studied by TG analysis of a Mn_2O_3 sample heating up to different temperatures ranging from 550 to 1000 ºC (Figure 7). In all cases, the sample was heated at 20 ºC/min up to the fixed temperature, followed by 4 hours of isothermal conditions at the studied temperature. All experiments were performed with an initial mass of 50 mg of Mn_2O_3, atmospheric pressure, and a gas flow of 50 cm^3/min of N_2.

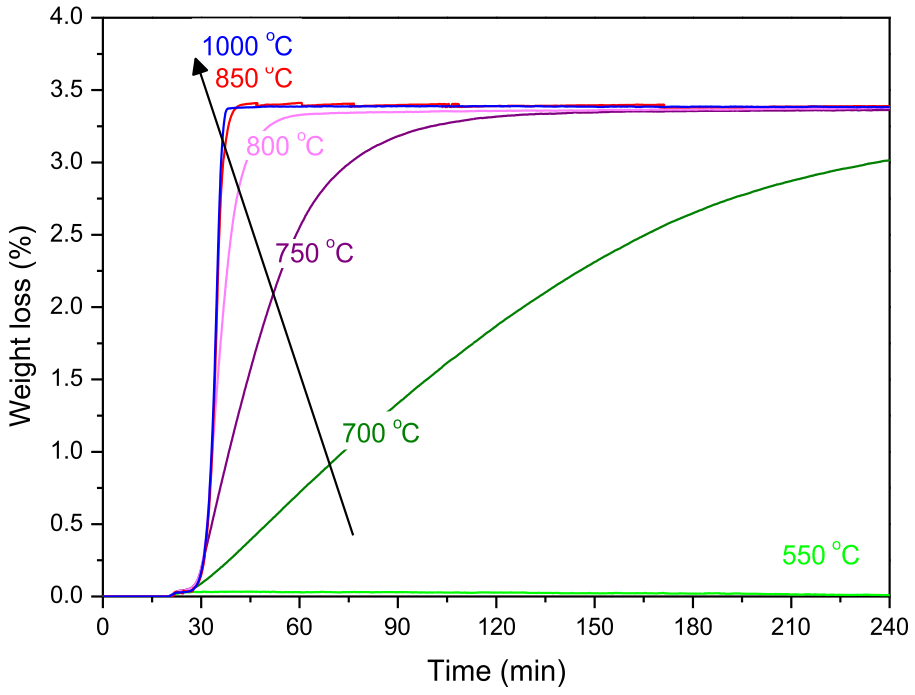

Figure 7. Thermogravimetric profiles of Mn_2O_3 thermal reduction to Mn_3O_4 at temperatures ranging from 550 to 1000 ºC (Heating rate: 20 ºC/min; initial temperature: 150 ºC; initial mass of Mn_2O_3: 50 mg; gas flow: 50 cm^3/min).

The results show that a negligible conversion is obtained at 550 ºC. For higher temperatures, a significant conversion is observed, being the reaction rate much higher as the temperature

increases until reaching a maximum at 850 – 1000 ºC. The experimental weight loss is in agreement with the theoretical value of 3.4 % calculated from the stochiometry of reaction 5.

Thermogravimetric analysis can be thermodynamically simulated following adequate assumptions derived of the non-static experimental set-up, in which a continuous flow of nitrogen is passing above the crucible with the sample. With this purpose, equilibrium conditions have been assumed between the solid and the free gas volume of the crucible, considering that the N_2 flow remove the O_2 released after each step of equilibrium calculation. The ratio between the gas volume in equilibrium and the gas flow used in the TG experiments leads to the time increment in the calculations and, considering the temperature program of the experiment, to the increase in the temperature required for the next equilibrium calculation to simulate the dynamic process. As an example, for an initial mass of 50 mg of Mn_2O_3, the free volume in the crucible is 0.11 cm^3, and considering a gas flow of 50 cm^3/min the interval for every equilibrium calculation step could be assumed to be 0.132 s or its equivalent 0.022 ºC if the heating ramp is 10 ºC/min. The theoretical weight loss can be calculated from the accumulated oxygen released to the gas phase and the initial amount of Mn_2O_3 according to equation 19.

$$\text{Weight loss (\%)} = \frac{\sum N_{O_2}^{eq} \times M_{O_2}}{N^0_{Mn_2O_3} \times M_{Mn_2O_3}} \times 100 \qquad (19)$$

Figure 8 shows the comparison of the experimental TG curve and the thermodynamically simulated equilibrium at this temperature program, starting with pure nitrogen in the gas phase. As it can be noticed, the experimental results are shifted to higher temperatures in comparison with the theoretical equilibrium (around 160-200 ºC corresponding to 8-10 min). The increase in the experimental temperature required for the reaction can be related to the reaction kinetics and O_2 diffusion effects neglected in the equilibrium calculation and usually controlling solid-state reactions, leading to the requirement of significant overequilibrium conditions as driving force for the process.

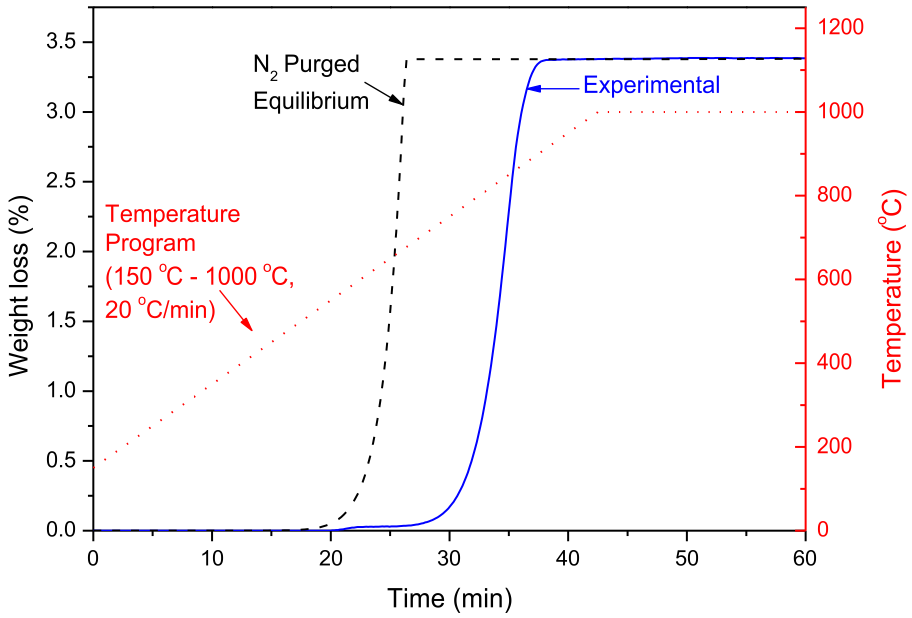

Figure 8. Experimental and simulated thermogravimetric curves for the thermal reduction of Mn_2O_3 to Mn_3O_4 at 1000 ºC (Heating rate: 20 ºC/min; initial temperature: 150 ºC; initial mass of Mn_2O_3: 50 mg; gas flow: 50 cm^3/min).

Thermogravimetric experiments at temperatures ranging from 1150 to 1500 ºC were also carried out to study the second reaction step of thermal reduction of Mn_3O_4 to MnO (reaction 6). In all the experiments a total conversion of the first reaction step is observed during the heating ramp (45 min corresponds to 1050 ºC). Differences appear in the second reaction step, from a negligible conversion at 1150 ºC to an increased reaction rate for higher temperatures, reaching the maximum theoretical weight loss of 10.1 %, that corresponds to the total conversion according to the stoichiometry of reactions 5 and 6. The simulated equilibrium curve at 1500 ºC is also included in Figure 9. As it happened in the first step, the experimental results are again shifted to higher temperatures (ca. 200 ºC) respect to the theoretical equilibrium as results of the critical influence of diffusion and chemical kinetics in the overall process, which is not considered in the equilibrium calculations.

Once established the influence of temperature in the system and the deviation from the thermodynamic equilibrium of the experimental system, the influence of operational variables of the process was also studied. Thus, different experiments at different flows of nitrogen were carried out and compared with the corresponding theoretical curves of the equilibrium composition (Figure 10).

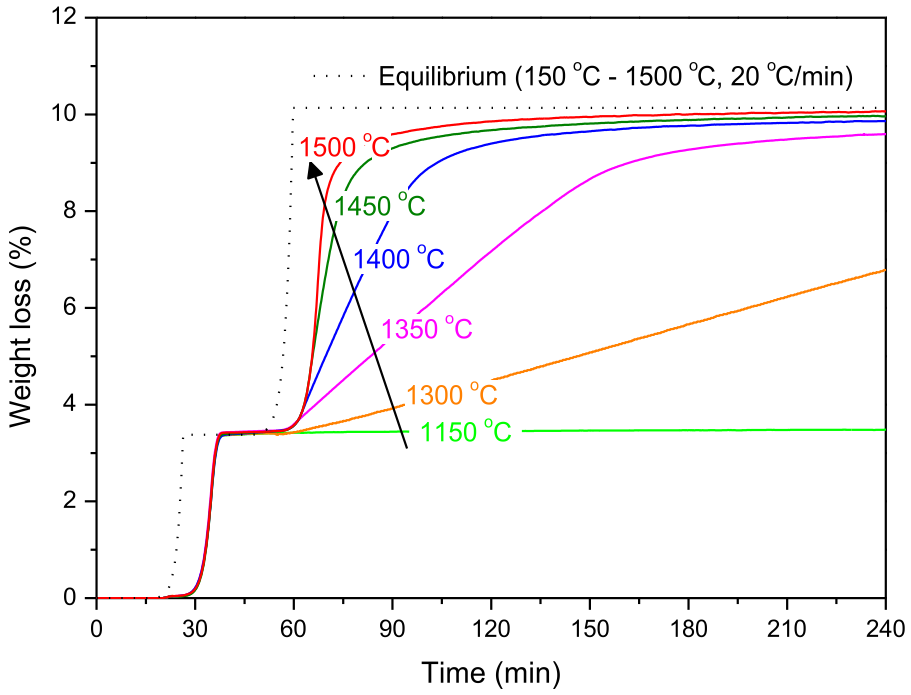

Figure 9. Thermogravimetric profiles of Mn_2O_3 thermal reduction at temperature ranging from 1150 to 1500 ºC and equilibrium curve obtained at 1500 ºC (Heating rate: 20 ºC/min; initial temperature: 150 ºC; initial mass of Mn_2O_3: 50 mg; gas flow: 50 cm^3/min).

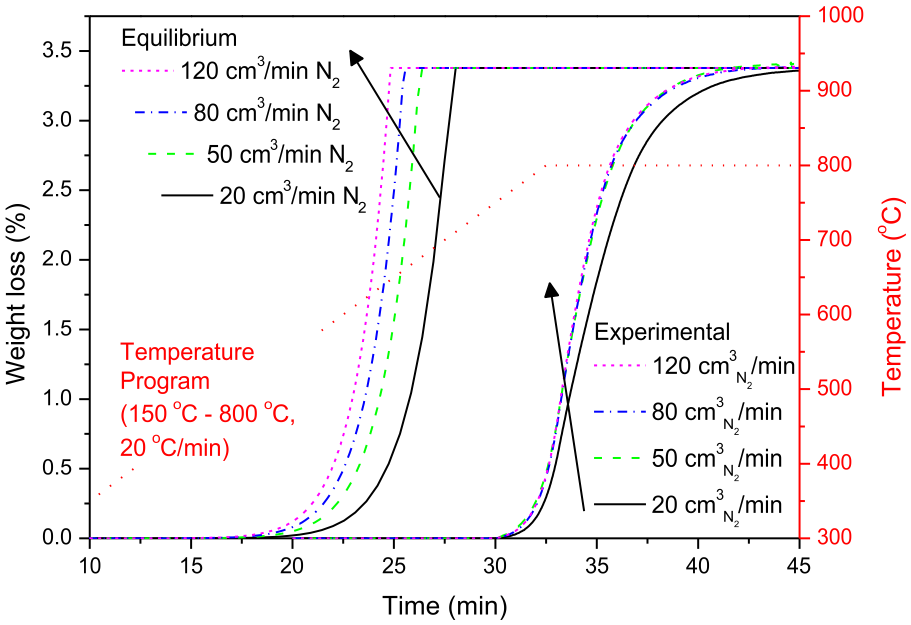

Figure 10. Influence of the flow of nitrogen in the thermal reduction of Mn_2O_3 to Mn_3O_4 at 800 ºC. Experimental and theoretical results (Heating rate: 20 ºC/min, initial temperature: 150 ºC; initial mass of Mn_2O_3: 50 mg).

Previous thermodynamic calculations represented in Figure 3 predicted a remarkable influence of the N_2/Mn_2O_3 molar ratio in the equilibrium composition. Thus, the higher the ratio the lower the temperature in which the reactions 5 and 6 proceed. Theoretical simulation of the thermogravimetric experiments at different flow of nitrogen results in a similar behaviour. However, the corresponding experimental thermogravimetric analysis shows that the influence of this variable is negligible for values higher than 50 cm^3/min, suggesting that the effect of this variable at low flow rate is more probably related to the external mass transport limitations in the diffusion of O_2 to the gas phase outside the crucible. Nevertheless, a complete reduction of Mn_2O_3 to Mn_3O_4 is obtained in all cases, although higher temperatures are required than those predicted by thermodynamic calculations.

Finally, the experimental effect of the initial loading of Mn_2O_3 was also studied and compared with the predictions of the equilibrium calculations (Figure 11). Experimental results and equilibrium calculations show that increasing the initial mass of manganese oxide displaces the temperatures in which the reduction takes place to higher values. From a theoretical point of view, an increase in the mass of the manganese oxide is accompanied with a decrease of the free gas volume for N_2 and O_2 equilibrium, and consequently a decrease in the gas/solid ratio that leads to higher predicted reaction temperatures (Figure 3). In the experimental system, the initial mass of the solid could also affect the reaction rate if the reaction were controlled by diffusion process into the solid, as usually happens in solid-state reactions. In any case, the simulation of the equilibrium successfully predict the effect of this variable, although in all cases the experimental results are shifted to higher temperatures as it happens along the previous discussion.

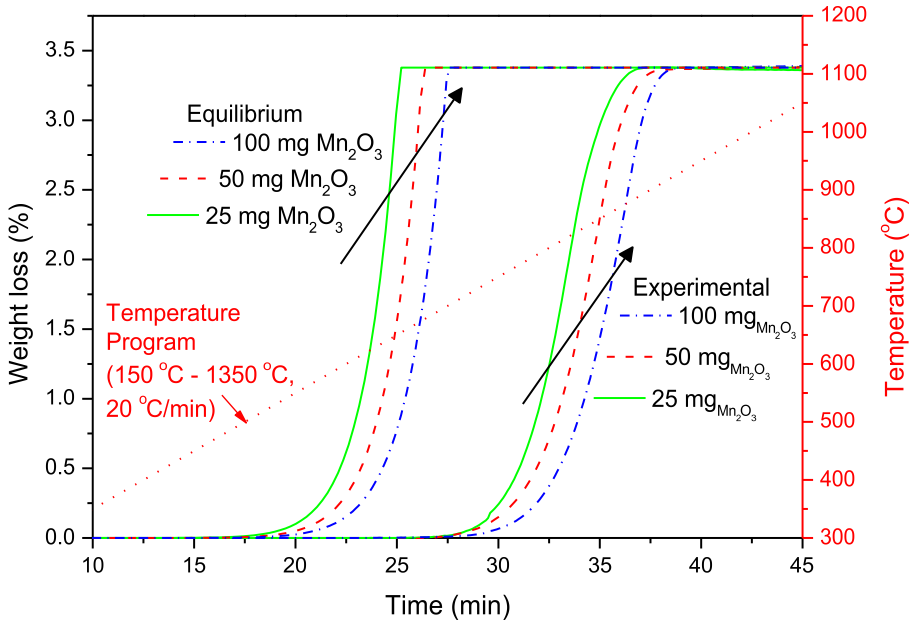

Figure 11. Influence of the flow of nitrogen in the thermal reduction of Mn_2O_3 to Mn_3O_4 at 1350 ºC. Experimental and theoretical results (Heating rate: 20 ºC/min, initial temperature: 150 ºC; gas flow: 50 cm^3/min).

3.3. Scaling-up and analysis of the solid products

The thermogravimetric analysis is a worthy tool for the validation of the theoretical studies. However, the response value is the weight loss of the sample along the thermal treatment, which is an indirect measurement of the conversion of Mn_2O_3 and Mn_3O_4 but not a direct determination. In that system, the analysis of the solids at the end of the process is hindered by the small amount of sample used in the experiments. For that reason, a complementary study at higher scale was performed, using a high temperature tubular furnace instead the thermogravimetric system. In this experimental set-up, higher amounts of Mn_2O_3 can be thermally reduced leading enough solid material products for a further characterization by XRD analyses. Pure samples of each manganese oxide were also used to validate the theoretical diffraction pattern of each crystalline phase.

Two sets of experiments at different temperature ranges were carried out to focus the study in each individual reaction step (550 to 1000 ºC to study the first reduction reaction, and 1150 to 1500 ºC for the second reaction to MnO). In all cases, 2 g of Mn_2O_3 where thermally reduced

under equivalent experimental conditions of temperature program and gas flow to solid ratio than those used in TG experiments.

Figures 12 and 13 show the XRD diffraction patterns of the final products as a function of the temperature of the treatment, together with the diffractograms of pure manganese oxide crystalline phases.

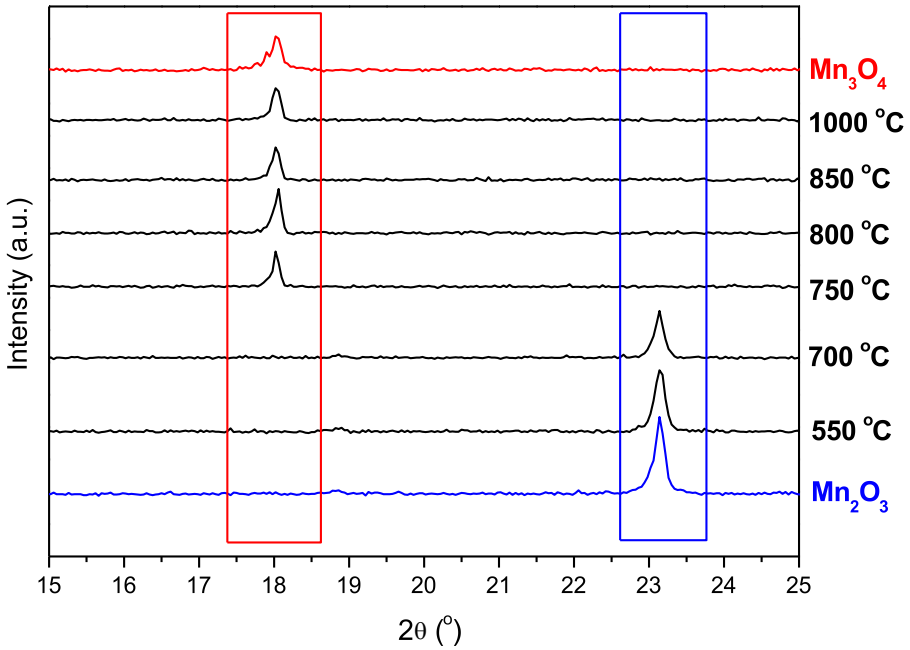

Figure 12. X-Ray diffraction patterns of Mn_2O_3 samples after heating in a range of temperatures of 550-1000 ºC (first thermal reduction of Mn_2O_3 to Mn_3O_4, reaction 5).

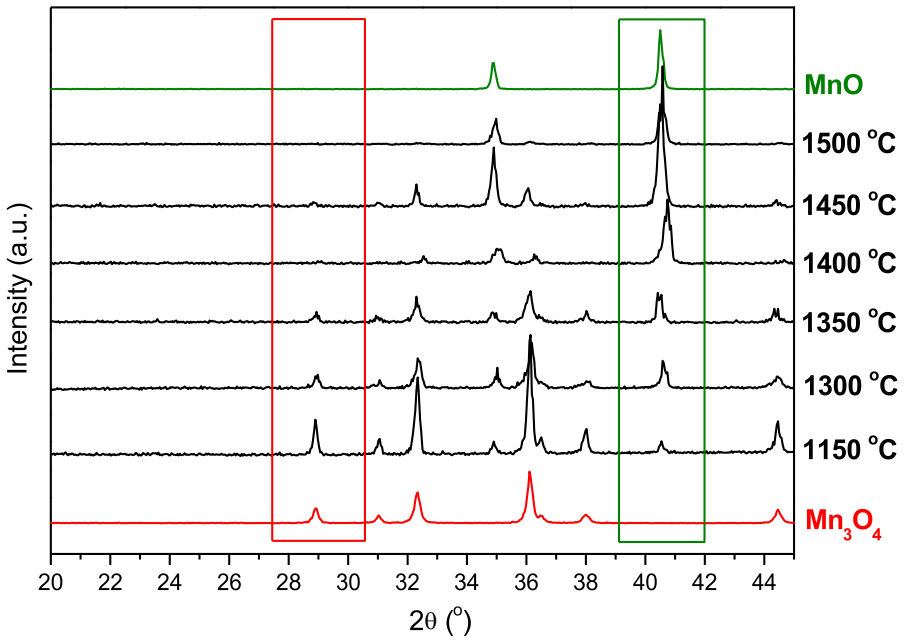

Figure 13. X-Ray diffraction patterns of Mn_2O_3 samples after thermal reduction in a range of temperatures of 1150-1500 ºC (second thermal reduction of Mn_3O_4 to MnO, reaction 6).

Experimental data at higher scale corroborate the previous thermodynamic simulation and TG results according to which both reaction steps take place sequentially at very different narrow temperature ranges. As it can be seen in Figure 12, the first thermal reduction of Mn_2O_3 to Mn_3O_4 takes place with a total conversion at between 700 and 750 ºC. Presence of MnO phase is not detected at 1000 ºC. The thermal reduction of Mn_3O_4 to MnO occurs during a wider range of temperatures, leading to mixtures of both oxides when working in the range from 1150 °C to 1350 °C, obtaining a total conversion to MnO when the initial Mn_2O_3 is treated at temperatures above 1400 ºC. Experimental temperatures for the phase transformations are in agreement with those previously obtained in theoretical studies and thermogravimetric analysis.

Mixture of solid phases was only detected in experiments between 1150 and 1450 ºC. In order to quantify the composition of the solid resultant of the thermal reduction of Mn_3O_4 to MnO, a calibration curve was prepared by the following method. According to the XRD patterns of pure compounds, typical an unequivocal peaks for Mn_3O_4 and MnO were selected for identification of phases in the solids (2θ = 29º and 41º , respectively). After that, different physical mixtures of pure Mn_3O_4 and MnO solid phases with known composition were prepared and analyzed by XRD, measuring the ratio between the area of both diffraction signals. The results were fitted to obtain a correlation between the composition of the prepared mixtures and the peaks area ratio. Table 1 summarizes the composition of the solids obtained at the different temperatures, by thermal reduction, taking into account this calibration curve. The results show that a total conversion is obtained at temperatures above 1400 ºC, which is in agreement with thermogravimetric results represented in Figure 9 and with the theoretical total conversions calculated in all cases from the thermodynamic study in gas flow regime.

Table 1. Composition of the solids after treatment at different temperatures

Temperature (ºC)	Mn_3O_4 (%)	MnO (%)
1000	100	0
1150	76	24
1300	32	68
1350	21	79
1400	< 1	> 99
1450	< 1	> 99
1500	0	100

4. Conclusions

The experimental data obtained both in a high temperature furnace and a thermobalance confirm the results of thermodynamic simulation according to which the thermal reduction of Mn_2O_3 takes place through a sequential mechanism of two reaction steps without simultaneous coexistence of the three manganese oxides solid phases involved in the process. The first step (reduction of Mn_2O_3 to Mn_3O_4) requires temperatures above 700 ºC to take place with acceptable kinetics, whereas the second reaction step (reduction of Mn_3O_4 to MnO) requires heating up above 1350 ºC to achieve a satisfactory reaction rate. Thermodynamic studies reveal a critical influence of the gas/solid ratio, pressure and composition of the gas in the equilibrium of the first step of the thermochemical cycle. Experimental results obtained in thermogravimetric analysis confirm thermodynamic calculations about the influence of those variables. It should be pointed out that experimental data show higher reaction temperatures that those predicted by equilibrium calculations, what means that overequilibrium conditions are required as driving force for the process, probably due to reaction kinetics and O_2 diffusion effects neglected in the equilibrium calculation and usually controlling solid-state reactions.

Summarizing all the results, it can be concluded that this work demonstrate that the first step of the Mn-oxide thermochemical cycle for hydrogen production can be carried out with total conversion at temperatures compatible with solar energy concentration devices. Those ranges

of temperatures are lower than those commonly reported in literature for the manganese oxide cycle obtained from theoretical and thermodynamic studies.

Acknowledgements

The authors wish to thank "Comunidad de Madrid" and "European Social Fund" for its financial support to the SOLGEMAC Project through the Programme of Activities between Research Groups (S2009/ENE-1617). Financial support of Ministerio de Ciencia e Innovación of Spain (Plan Nacional de Investigación Científica, Desarrollo e Innovación Tecnológica 2008-20) and Fondo Europeo de Desarrollo Regional (FEDER) through the program PSE-H2RENOV SP4-HYTOWER (PSE-120000-2009-3) is also gratefully acknowledged. C. Herradón also thanks Universidad Rey Juan Carlos for its PhD grant.

References

[1] Campen A, Mondal K, Wiltowski T. Separation of hydrogen from syngas using a regenerative system. International Journal of Hydrogen Energy 2008; 33:332-339.

[2] Pregger T, Graf D, Krewitt W, Sattler C, Roeb M, Möller S. Prospects of solar thermal hydrogen production processes. International Journal of Hydrogen Energy 2009; 34:4256-4267.

[3] Perkins C, Weimer AW. Likely near-term solar-thermal water splitting technologies. International Journal of Hydrogen Energy 2004; 29:1587-1599.

[4] Kogan A, Spiegler E, Wolfshtein M. Direct solar thermal splitting of water and on-site separation of the products. III. Improvement of reactor efficiency by steam entrainment. International Journal of Hydrogen Energy 2000; 25:739-745.

[5] Kogan A. Direct solar thermal splitting of water and on-site separation of the products - IV. Development of porous ceramic membranes for a solar thermal water-splitting reactor. International Journal of Hydrogen Energy 2000; 25:1043-1050.

[6] Ohya H, Yatabe M, Aihara M, Negishi Y, Takeuchi T. Feasibility of hydrogen production above 2500 K by direct thermal decomposition reaction in membrane reactor using solar energy. International Journal of Hydrogen Energy 2002; 27:369-376.

[7] Baykara SZ. Experimental solar water thermolysis. International Journal of Hydrogen Energy 2004; 29:1459-1469.

[8] Atkin I, Elder RH, Priestman GH, Sinclair DC, Allen RWK. High temperature oxygen separation for the sulphur family of thermochemical cycles - part I: Membrane selection and flux testing. International Journal of Hydrogen Energy, in press doi:10.1016/j.ijhydene.2011.05.113.

[9] Lima H, Oyama ST. Hydrogen selective thin palladium–copper composite membranes on alumina supports. Journal of Membrane Science 2011; 378:179-185.

[10] Perret R, Chen Y, Besenbruch G, Diver R, Weimer A, Lewandowski A, Miller E. Solar Hydrogen Generation Research. DOE Hydrogen Program 2005, Annual Progress Report. *http://www.hydrogen.energy.gov/*

[11] Charvin P, Abanades S, Lemort F, Gilles F. Analysis of solar chemicals processes for hydrogen production from water splitting thermochemical cycles. Energy conversion and management 2009; 49:1547-1556.

[12] Steinfeld A, Sanders S, Palumbo R. Design aspects of solar thermochemical engineering - A case of study: Two-step water-splitting cycle using the Fe_3O_4/FeO redox system. Solar Energy 1999; 65:43-53.

[13] Abanades S, Flamant G. Thermochemical hydrogen production from a two-stpe solar-driven water-splitting cycle based on cerium oxides. Solar Energy 2006; 80:1611-1623.

[14] Müller R, Steinfeld A. H_2O-splitting thermochemical cycle based on ZnO/Zn-redox: Quenching the effluents from the ZnO dissociation. Chemical Engineering Science 2008; 63:217-227.

[15] Abanades S, Charvin P, Lemont F, Flamnat G. Novel two-step SnO_2/SnO water-splitting cycle for solar thermochemical production of hydrogen. International Journal of Hydrogen Energy 2008; 33:6021-6030.

[16] Meier A, Steinfeld A. Solar thermochemical production of fuels. Advances in Science and Technology 2010; 74:303-312.

[17] Schunk LO, Haeberling P, Wepf S, Wuillemin D, Meier A, Steinfeld A. A Receiver-Reactor for the Solar Thermal Dissociation of Zinc Oxide. Journal of Solar Energy Engineering 2008; 130:021009-1-021009-6.

[18] Tamaura Y, Steinfeld A, Kuhn P, Ehrensberger K. Production of solar hydrogen by a novel, 2 step, water-splitting thermochemical cycle. Energy 1995; 20:325-330.

[19] Fresno F, Fernandez-Saavedra R, Gómez-Mancebo MB, Vidal A, Sánchez M, Rucandio MI, Quejido AJ, Romero M. Solar hydrogen production by two-step thermochemical cycles: Evaluation of the activity of commercial ferrites. International Journal of Hydrogen Energy 2009; 34:2918-2924.

[20] Kodama T, Gokon N, Yamamoto R. Thermochemical two-step water spliting by ZrO_2-supported $Ni_xFe_{3-x}O_4$ for solar hydrogen production. Solar Energy 2008; 82:73-79.

[21] Gokon N, Kodama T, Imaizumi N, Umeda J, Seo T. Ferrite/Zirconia-coated foam device prepared by spin coating for solar demonstration of thermochemical water-plitting. International Journal of Hydrogen Energy 2011; 36: 2014-2028.

[22] Le Gal A, Abanades S. Catalytic investigation of ceria-zirconia solid solutions for solar hydrogen production. International Journal of Hydrogen Energy 2011; 36:4739-4748.

[23] Meng QL, Lee CI, Kaneko H, Tamaura Y. Solar thermochemical process for hydrogen production via two-step water splitting cycle based on $Ce_{1-x}Pr_xO_{1-\delta}$ redox reaction. Thermochimica Acta, in press doi:10.1016/j.tca.2011.01.028.

[24] Charvin P, Abanades S, Lemort F, Flamant G. Hydrogen production by Three-Step

Thermochemical Cycle Using Hydroxides and Metal Oxide Systems. Energy & Fuels 2007; 21:2919-2928.

[25] Sturzenegger M, Nüesch P. Efficiency analysis for a manganese-oxide-based thermochemical cycle. Energy 1999; 24:959-970.

[26] Francis TM, Lichty PR, Weimer AW. Manganese oxide dissociation kinetics for the Mn_2O_3 thermochemical water-splitting cycle. Part I: Experimental. Chemical Engineering Science 2010; 65:3709-3717.

[27] Kreider PB, Funke HH, Cuche K, Schmidt M, Steinfeld A, Weimer AW. Manganese oxide based thermochemical hydrogen production cycle. International Journal of Hydrogen Energy 2011; 36: 7028-7037.